International Journal of Applied Earth Observation and Geoinformation 59 (2017) 167–174

Contents lists available at ScienceDirect

International Journal of Applied Earth Observation and Geoinformation

journal homepage: www.elsevier.com/locate/jag

Shape indexes for semi-automated detection of windbreaks in thematic tree cover maps from the central United States

Greg C. Liknes[a,*], Dacia M. Meneguzzo[a], Todd A. Kellerman[b]

[a] USDA Forest Service, Northern Research Station, 1992 Folwell Avenue, Saint Paul, MN 55108, USA
[b] USDA National Agroforestry Center, 1945 North 38th Street, UNL-East Campus, Lincoln, NE 68583, USA

ARTICLE INFO

Article history:
Received 17 October 2016
Received in revised form 8 March 2017
Accepted 10 March 2017

Keywords:
Windbreaks
Image morphology
Agroforestry
Shape-based classification

ABSTRACT

Windbreaks are an important ecological resource across the large expanse of agricultural land in the central United States and are often planted in straight-line or L-shaped configurations to serve specific functions. As high-resolution (i.e., <5 m) land cover datasets become more available for these areas, semi- or fully-automated methods for distinguishing windbreaks from other patches of trees are needed for use with thematic raster datasets. To address this need, we created three shape indexes: a morphology-based index that we have named the Straight and Narrow Feature Index (SNFI), a windbreak sinuosity index, and an area index indicating the occupied fractional area of a bounding box. The indexes were tested in two study areas: (1) a riparian area dominated by sinuous bands of trees but mixed with row crop agriculture and (2) an agricultural area with a mix of straight-line and L-shaped windbreaks. In the riparian area, a Kruskall–Wallis rank sum test indicated class differences for all three indexes, and pairwise comparisons indicate windbreaks and riparian trees are separable using any of the three indexes. SNFI also produced significant differences between windbreaks oriented in different directions (east–west vs. north–south). In the agricultural area, the Kruskall–Wallis rank sum test indicated differences between classes for all three indexes, and pairwise comparisons show that all class pairs have significant differences for at least one index, with the exception of L-shaped windbreaks vs. non-windbreak tree patches. We also used classification trees to objectively assign representative samples of tree patches to classes using both single indexes and multiple indexes. Classes were correctly assigned for more than 90% of the samples in both the riparian and agricultural study areas. In the riparian area, combining indexes did not improve accuracy compared to using SNFI alone, whereas in the agricultural area, combining the three indexes produced the best result. Thematic datasets derived from high-resolution imagery are becoming more available, and extracting useful information can be a challenge, partly due to the large amount of data to assess. Calculating the three shape indexes presented can assist with efficient identification of candidate windbreaks and as such, hold good promise for value-added analysis of tree function in the central United States.

Published by Elsevier B.V.

1. Introduction

Windbreaks are an important ecological resource across the large expanse of agricultural land in the central United States and are often planted in a particular location to provide a specific function (Brandle et al., 2004). For example, a long narrow row of trees adjacent to a farm field protects crops and soil from desiccating winds, thus enhancing crop productivity and reducing soil erosion (U.S. Dept. of Agriculture, 2012). However, anecdotal evidence indicates that many windbreaks are being removed from the landscape due to high land and crop prices, changes in farming practices, and age-related decline in windbreak condition. Quantifying changes in the resource for a large area is challenging due to lack of objective and consistent information. While efforts are being made to map tree cover from high-resolution imagery (e.g., Liknes et al., 2010; Basu et al., 2015), efficient methods are needed to distinguish windbreaks from spectrally similar patches of trees serving other functions on the landscape, such as buffering water bodies.

A number of classification methods have been developed to exploit spatial relationships in addition to utilizing spectral information of target pixels. In the early days of Landsat satellites, the ECHO classification method incorporated neighborhood information for each pixel (Kettig and Landgrebe, 1976). More recently,

* Corresponding author.
E-mail addresses: gliknes@fs.fed.us (G.C. Liknes), dmeneguzzo@fs.fed.us (D.M. Meneguzzo), tkellerman@fs.fed.us (T.A. Kellerman).

http://dx.doi.org/10.1016/j.jag.2017.03.005
0303-2434/Published by Elsevier B.V.

the Getis statistic has been paired with a random forests classifier (Breiman, 2001) to improve land cover classification using Landsat ETM+ imagery (Ghimire et al., 2010). With increasing availability of higher resolution imagery (e.g., <5 m), there are a growing number of methods that rely on the shape of landscape features, rather than a pixel neighborhood, for classification.

Man-made features, such as those in an urban environment often have very distinctive shapes and sizes and have been classified using panchromatic imagery, a differential morphological profile (Benediktsson et al., 2003), and a fuzzy membership classifier (Chanussot et al., 2006). These methods use variations of morphological operations, such as opening and closing, to extract information about features in an image. Other methods rely on detecting known geometry of target features; for example, the Regular Shape Similarity Index makes use of the relationship between a feature's area and the area of a minimum bounding polygon for that same feature (Sun et al., 2015). Geometric indexes like compactness, roundness, and convexivity have been used with good success to distinguish different types of water bodies that were first classified from Landsat spectral information (van der Werff and van der Meer, 2008).

There's a large body of literature addressing a specific case of shape-based classification, namely linear feature detection. Quackenbush (2004) provides a review of linear feature detection methods and categorizes approaches into several groups, one of which is morphology. These methods are appealing in that they are relatively easy to implement using existing functions in many GIS and remote sensing software packages. We note that some of the methods presented in the literature detect narrow features; that is, both linear and curvilinear features may be identified. Linear feature detection methods often focus on application directly to aerial photography or satellite imagery and less on identifying linear features in thematic maps (i.e., classified imagery). However, Morphological Spatial Pattern Analysis (MSPA, Soille and Vogt, 2009) was developed for use with thematic outputs and has been used to analyze forest fragmentation (Vogt et al., 2007; Riitters et al., 2009), landscape corridors (Vogt et al., 2007), and more. MSPA categorizes spatial patterns in thematic maps including core, edge, islet, perforation, bridges, loops, and branches. Several of these categories are narrow features (such as bridges and branches) that may not necessarily be long or straight. Because the distinction between curvilinear and linear features may be important for determining the type of landscape feature, the selection of the appropriate linear detection method is a vital component for extracting information from mapped datasets.

Aksoy et al. (2010) provides a comprehensive method for automatic detection of woody linear features in agricultural landscapes starting from high resolution imagery. Using Quickbird imagery as an example, woody vegetation was differentiated from other vegetation, candidate features were skeletonized, and linear regression on the skeleton vertices produces an intercept and slope that are evaluated in order to determine if the features are linear (straight). While the method performed well at identifying linear woody features, we chose to explore whether or not relatively simple shape metrics that can be calculated using basic focal and zonal raster processing functions could be constructed for the purpose of identifying linear tree features in the central United States. These features are easily identified in aerial or satellite images by their straight and narrow shapes and their north–south or east–west orientation (Fig. 1).

We consider a specific scenario in which tree cover has been mapped using high-resolution (1-m) aerial photography and an object-based image analysis (OBIA) procedure that groups similar pixels into image objects that represent single or multiple tree crowns. Object-based classification is ideally suited to this type of application with high-resolution imagery because it can be applied in such a way that contiguous patches are maintained (Meneguzzo et al., 2013); in this case it is beneficial to consider each windbreak as a single unit even if there are gaps between tree crowns. Our objective is to develop a method that can help provide previously unavailable information about the extent, location, and function of trees in agricultural landscapes of the central United States. In order to achieve this objective, our goal for the method presented is to classify tree cover into various categories based on their shape with particular emphasis on windbreaks and riparian corridors. Furthermore, we aim to produce a method that is readily compatible with functions available in GIS and remote sensing software packages and that is efficient enough to apply over large areas such as a county in the central United States (a political subdivision of a state that may typically be on the order of 2000 km^2).

Fig. 1. Typical agricultural landscape in the central United States with linear planted windbreaks.
(Image source: U.S. Department of Agriculture National Agriculture Imagery Program).

2. Methods

2.1. Tree cover map

A four-class land cover dataset of Nebraska, USA based on 2009 aerial photography from the U.S. Department of Agriculture's National Agriculture Imagery Program was used for this study. Two study areas were selected: one along the northern border of Antelope County and partly in adjacent Knox County, and the second along Antelope County's eastern border and partly in Pierce County (Fig. 2). These areas were chosen because they contain an extensive network of windbreaks and riparian corridors, as well as other small groupings of trees. The dataset was created using object-based image analysis and was delivered as a raster output product. We converted the data to a binary raster with pixels representing tree cover set to foreground pixels (value = 1) and all other pixels set to the background (value = 0) (Fig. 3a). A region group operation was applied to create a companion dataset for which each contiguous cluster of trees had a unique identifier, which we will refer to hereafter as zones (Fig. 3b).

2.2. Morphological method

A hit-or-miss transform can be applied to an image to determine which areas match a shape specified by a structuring element, or kernel (Dougherty and Lotufo, 2003). This also requires the user to specify the size of the kernel, and for best results, should match the

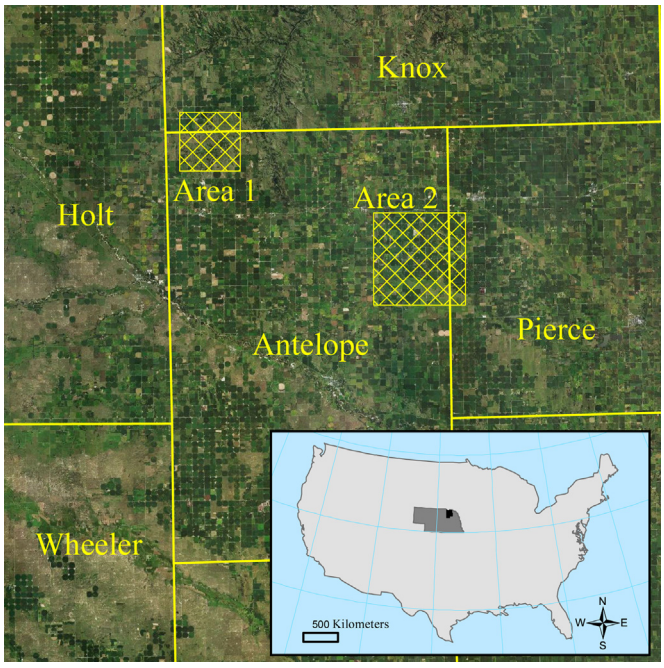

Fig. 2. Location of study areas in northeastern Nebraska, USA, shown as yellow, cross-hatched areas in Antelope, Knox, and Pierce Counties. The inset map depicts the location of the counties (black) within Nebraska (dark gray), USA. (For interpretation of the references to color in this figure legend, the reader is referred to the web version of the article.)

(Image source: U.S. Department of Agriculture National Agriculture Imagery Program).

size of the features of interest. We apply a version of this concept wherein the kernel is only a single pixel in height or width and a morphological erosion is applied using these narrow kernels oriented in both major directions, north–south and east–west (Fig. 4). The longer kernel dimension relates to a maximum width expected for a linear feature. In our case, we used a kernel dimension of 37 m which is similar to the threshold (36.6 m) for minimum width of a patch of forest in the definition of forest land within the national forest inventory in the United States (O'Connell et al., 2014).

For each erosion operation, the sum of the remaining pixels within each zone was determined. We then calculated an index from these zonal summations that we have termed the Straight and Narrow Feature Index (SNFI):

$$\mathrm{SNFI} = \frac{\sum_z f\theta s_{(1\times m)} - \sum_z f\theta s_{(m\times 1)}}{\sum_z f\theta s_{(1\times m)} + \sum_z f\theta s_{(m\times 1)}}$$

where z indicates the summation is conducted over all pixels in a zone after the erosion (θ), is applied to a binary image (f) using structuring elements (s) with a single row and user-defined number of columns ($1 \times m$) and a single column and user-defined number of rows ($m \times 1$).

A simpler interpretation of this index is the difference in the proportion of narrow templates oriented in the two major directions that "fit" within the mapped tree zones. Because a normalized difference is used, the area of the zone cancels out, and the index can be calculated from the sum (or count) of pixels that remain after the two erosions are applied. The index ranges from −1 to +1, and narrow features oriented with the longer dimension along with y-axis (north/south) have values near +1, features oriented east/west have values near −1, and features that have characteristics of both fall in the middle of the range.

2.3. Geometric methods

The SNFI uses morphological concepts to identify features less than a specified width that are oriented mostly north/south or east/west (as is the case for windbreaks in the central U.S.). To a degree, it provides information about the straightness of each feature since more complex features would be less likely to contain the long, straight kernel in either dimension. As a complementary index, we also wanted to quantify the deviation of mapped tree zones from rectangular. Borrowing the concept of sinuosity from geomorphology (e.g., Mueller, 1968), we developed a simplified windbreak sinuosity index. Each zone's perimeter is compared to the Euclidean distance between the lower left and upper right corner of the zone's bounding box. While a more precise calculation is straightforward using vector data, this approximation works natively on raster data, can be implemented with existing GIS functions, and executes quickly for large rasters:

$$\text{Windbreak sinuosity index} = \frac{\frac{1}{2}\text{Perimeter}}{\sqrt{(\max_y - \min_y)^2 + (\max_x - \min_x)^2}}$$

where all variables are calculated for each zone.

Consider the sinuosity index for rectangles of increasing length-to-width ratio. For a rectangle with a 1:1 ratio (i.e., a square), the sinuosity index is 1.4, and the index approaches a value of 1 as the ratio increases. Compact features or features with irregular borders will exhibit higher values of the index (Fig. 5) (e.g., the ratio of the half circumference of a circle to the diameter is $\pi/2 = 1.57$).

There are also a number of narrow windbreaks planted in an "L" configuration across the central United States. In order to identify these features, we consider the ratio between the area of a zone and the area of the zone's bounding rectangle. This ratio should be

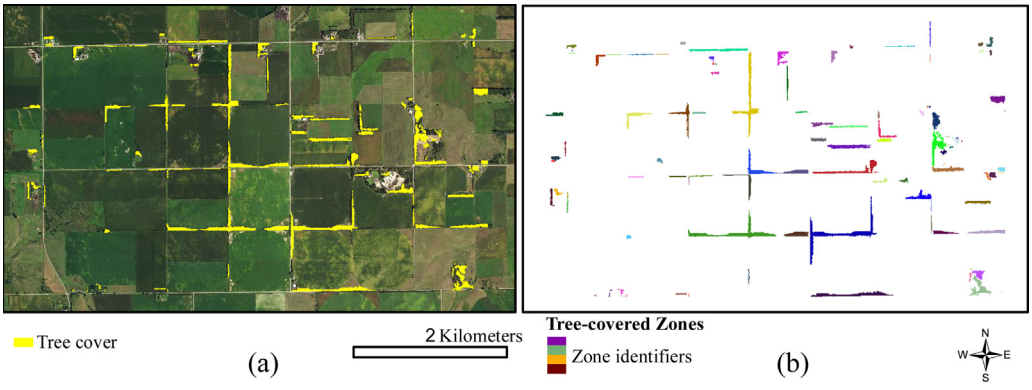

Fig. 3. (a) A subset of a land cover map from Nebraska, USA that has been converted to a binary tree cover map. (b) Each contiguous cluster of trees has been assigned a unique zone identifier.

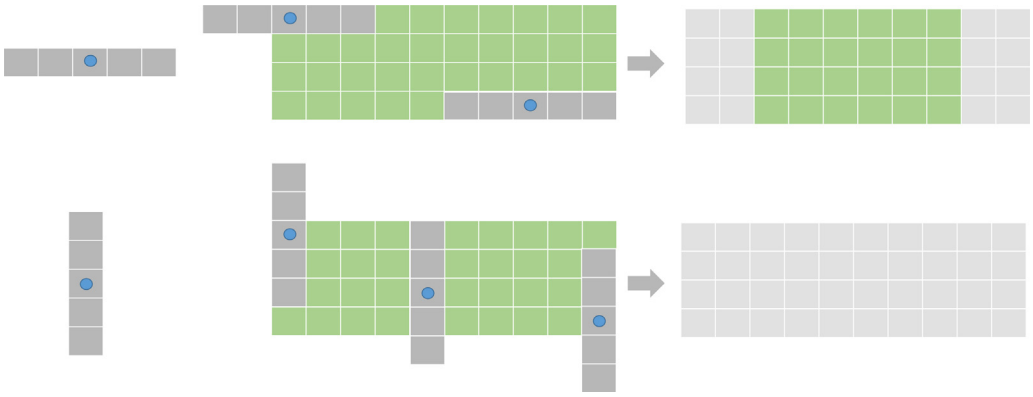

Fig. 4. Example of a morphological erosion of an idealized windbreak (middle, green) using single row and single column kernels (left, dark gray). The kernel is passed over each cell of the windbreak, and if the kernel fits completely within the windbreak, the cell coincident with the kernel center (indicated by the blue dot) retains the foreground value. If the kernel does not remain within the windbreak area, the cell is turned to the background value (right, light gray). The horizontal kernel erodes the left and right edges of the windbreak, leaving the interior intact (upper right). The vertical kernel erodes the entire windbreak, and no foreground pixels remain (lower right). (For interpretation of the references to color in this figure legend, the reader is referred to the web version of the article.)

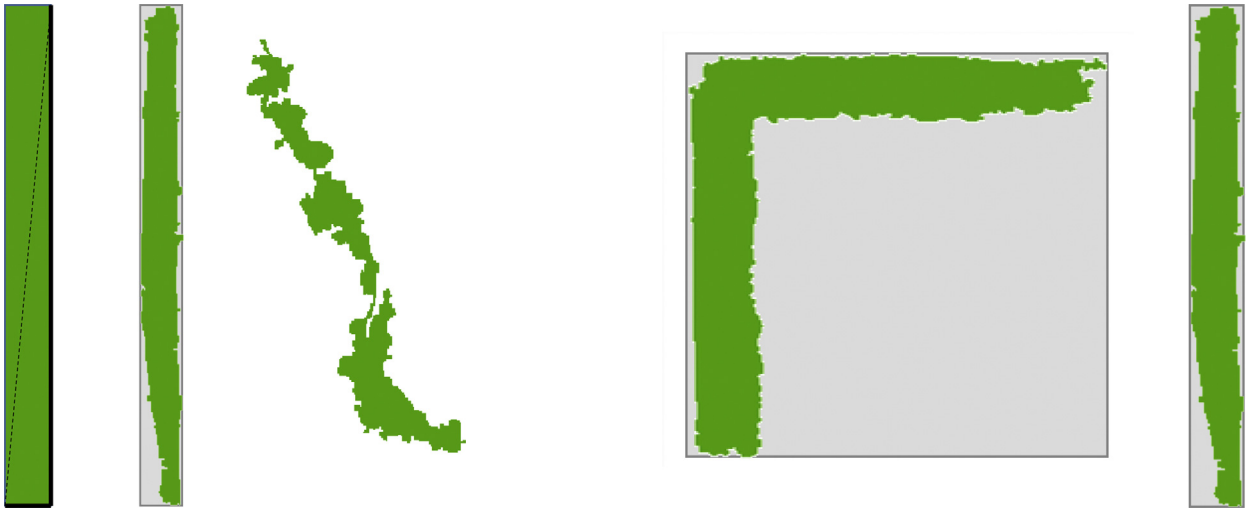

Fig. 5. Example of a sinuosity index for an idealized windbreak with 10:1 length to width ratio (left), along with two examples extracted from study area 1: a windbreak (middle) and trees in a riparian corridor (right). The index is the ratio of the half perimeter (heavy line around right and bottom of the idealized windbreak) to the distance between the lower left corner and upper right corner (dashed line). The idealized windbreak has a windbreak sinuosity index value of 1.09 (left), and the mapped windbreak and riparian corridor have values of 1.24 (middle) and 2.21 (right).

Fig. 6. Illustration of an area index for L-shaped and north–south windbreaks from study area 2. The index is calculated by dividing each feature's area (in green) by the area of the bounding rectangle (shaded background). In this case, the area index is 0.26 for the L-shaped windbreak and 0.75 for the north–south windbreak. (For interpretation of the references to color in this figure legend, the reader is referred to the web version of the article.)

small for L-shaped windbreaks relative to straight line windbreaks (Fig. 6).

$$\text{Area index} = \frac{\text{Area}_z}{\text{Area}_{\text{rect}}}$$

where Area_z is the area of foreground pixels in a zone and $\text{Area}_{\text{rect}}$ is the area of the zone's bounding rectangle.

2.4. Analyses

We selected two study areas within the county – one area is dominated by narrow, sinuous bands of tree cover in a riparian area adjacent to farm fields, and the other is predominantly agricultural with a large number of both straight line and L-shaped windbreaks. Indexes were calculated using ArcGIS™ software and were assigned to the corresponding zone.

For the riparian study area, we were interested in how well the indexes could help distinguish sinuous riparian tree cover from straight-line windbreaks. We manually labeled representative zones ($n = 37$) as either "north–south windbreak", "east–west windbreak" or "other" (e.g., riparian corridors or other non-windbreaks). Because there were few L-shaped windbreaks in the area, we did not assign that class. We assessed the separability of these classes using a Kruskall–Wallis rank sum test, and where appropriate followed with a pairwise comparison (Siegel and Castellan, 1988) using the *pgirmess* package in R (Giraudoux, 2016).

In order to determine the thresholds for each index that produce the most accurate separation between windbreaks and non-windbreaks, we applied a classification tree using the *tree* package in the R statistical computing environment (Ripley, 2016). We also generated a classification tree using all three of the indexes and compared to the accuracy obtained using the single index trees. We note that east–west and north–south windbreaks were labeled separately only to demonstrate the functionality of SNFI. For the classification tree analysis, we grouped these two classes together since the other two indexes are not designed to distinguish the directional orientation of windbreaks, and the objective for the riparian study area was simply to separate sinuous from straight-line tree features.

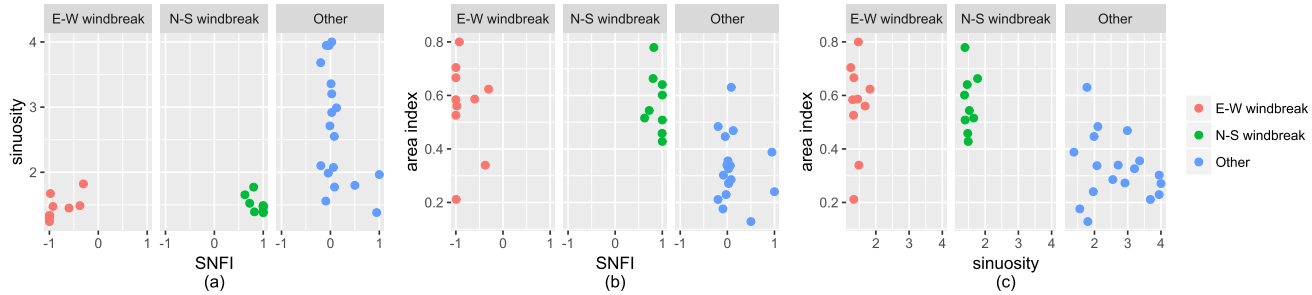

Fig. 7. Pairwise scatterplots of three shape indexes – a windbreak sinuosity index vs. the Straight-and-Narrow Feature Index (SNFI) (a), an area index vs. SNFI (b), and an area index vs. a windbreak sinuosity index (c) – for east–west windbreaks (E–W), north–south windbreaks (N–S), and non-windbreak tree-covered areas (Other) located in Nebraska, USA.

Table 1
Results of a Kruskall–Wallis rank sum test for differences between tree classes with respect to three shape metrics – the Straight-and-Narrow Feature Index (SNFI), a sinuosity index, and an area index.

Variable	Chi-squared	df	*p*
SNFI	28.387	2	<0.01
Sinuosity index	21.854	2	<0.01
Area index	16.341	2	<0.01

Table 2
Results of post hoc pairwise comparison tests for three shape metrics. The check mark indicates statistically significant ($p < 0.05$) differences between classes.

Class pairing	SNFI	Sinuosity index	Area index
E–W/N–S	√		
E–W/Other	√	√	√
N–S/Other	√	√	√

In the agriculture study area, we repeated a similar analysis with a few differences. We manually labeled representative zones ($n = 53$) as "north–south windbreak", "east–west windbreak", "L-shaped windbreak", or "other". We calculated the three indexes and assigned them to each zone. We assessed separability using the Kruskall–Wallis rank sum test and pairwise comparisons. We again used classification trees to examine the thresholds that provided the best labeling for the four classes, as well as examining the accuracy for single and multiple variable models.

3. Results

In the riparian area, most of the east–west (E–W) windbreak samples had SNFI values near −1, and the north–south (N–S) windbreaks were all very close to a value of +1 (Fig. 7a and b). With respect to sinuosity, the windbreaks generally had low values while those in the "other" category were higher on average but also covered a large range of values (Fig. 7a and c). For the area index, the windbreaks had higher values than the "other" category (Fig. 7b and c). The Kruskall–Wallis rank sum test indicated that there were differences between at least one pairing of classes (Table 1). The post hoc pairwise comparisons indicated that the differences were significant ($p < 0.05$) for SNFI among all class pairs and significant for sinuosity and area between the straight-line windbreaks and other category but not for the E–W/N–S pairing (Table 2).

The classification tree using only SNFI as a predictor indicated values less than −0.252 and greater than 0.562 could be used to discriminate windbreaks from the "other" category. The classification tree using those values correctly identified 94.6% (35/37) of the manually labeled features. The sinuosity classification tree indicated features with a sinuosity less than 1.77 should be labeled as windbreaks and that tree was able to correctly label 91.9% (34/37) of

Table 3
Results of a rank sum test for differences between tree classes with respect to three shape metrics – the Straight-and-Narrow Feature Index (SNFI), a sinuosity index, and an area index.

Variable	Chi-squared	df	*p*
SNFI	37.695	3	<0.01
Sinuousity	17.266	3	<0.01
Area index	21.639	3	<0.01

Table 4
Results of post hoc pairwise comparison tests for three shape metrics. The check mark indicates statistically significant ($p < 0.05$) differences between classes.

Class pairing	SNFI	Sinuosity index	Area index
E–W/N–S	√		
E–W/L-shaped			√
E–W/Other	√	√	
N–S/L-shaped	√		√
N–S/Other	√	√	
L-shaped/Other			

the zones. The classification tree indicated zones with an area index greater than 0.496 should be labeled as windbreaks, and the accuracy was 86.5% (32/37). The classification tree using all indexes as predictors did not result in an improvement in accuracy compared to the single models (91.9%). The indexes and the prediction from the full model appear in Fig. 8.

In the agricultural area, the values of SNFI for north–south windbreaks are close to +1, and values for east–west windbreaks are near −1 (Fig. 9). The area index of L-shaped windbreaks is generally lower than that of the N–S/E–W windbreaks, but the other category spans a large range of the index. One notable difference for the agricultural area is the reduced separability of classes in the sinuosity index relative to the riparian study area.

In the agricultural area, the Kruskall–Wallis rank sum test indicated significant ($p < 0.05$) differences between at least one pair of classes with respect to all of the indexes (Table 3). The pairwise comparisons indicated significant differences ($p < 0.05$) for all class pairings for at least one index, with the exception of L-shaped windbreaks vs. the other category (Table 4).

As with the riparian area, single variable classification trees were created. For SNFI, the threshold for N–S windbreaks is 0.727 and for E–W windbreaks is −0.696. The SNFI classification tree correctly classified 84.9% (45/53) of the manually labeled zones. For the sinuosity index, all N–S/E–W windbreaks had a sinuosity below 1.68. The sinuosity classification tree correctly classified 58.5% (31/53) of the manually labeled zones. For the area index, N–S/E–W windbreaks had values that exceeded 0.31 and the classification tree correctly classified 67.9% (36/53) of the zones. The full classification tree that included all three indexes (Fig. 10) performed significantly better than the single variable trees, correctly classifying

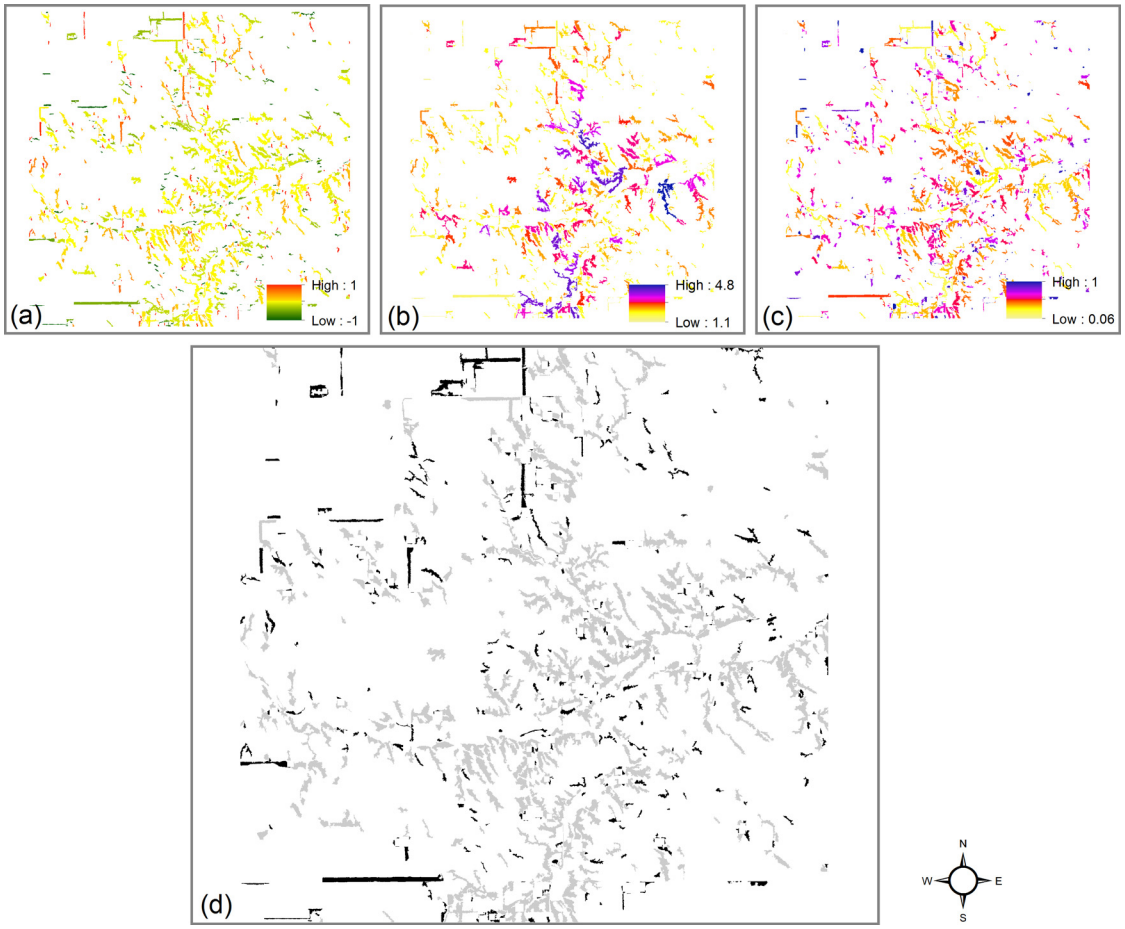

Fig. 8. Three shape indexes, SNFI (a), windbreak sinuosity (b), and area index (c) for tree features in a riparian study area in Nebraska, USA. Tree classes were labeled by a classification tree using the three shape indexes as inputs with windbreaks in black and other features in gray (d).

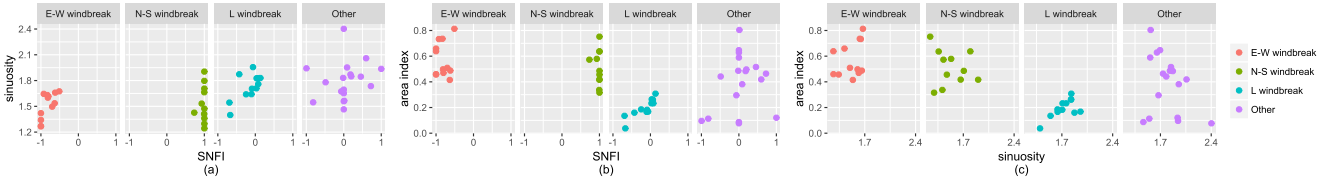

Fig. 9. Pairwise scatterplots of three shape indexes – a windbreak sinuosity index vs. the Straight-and-Narrow Feature Index (SNFI) (a), an area index vs. SNFI (b), and an area index vs. a windbreak sinuosity index (c) – for east–west windbreaks (E–W), north–south windbreaks (N–S), L-shaped windbreaks, and non-windbreak tree-covered areas (Other) located in Nebraska, USA.

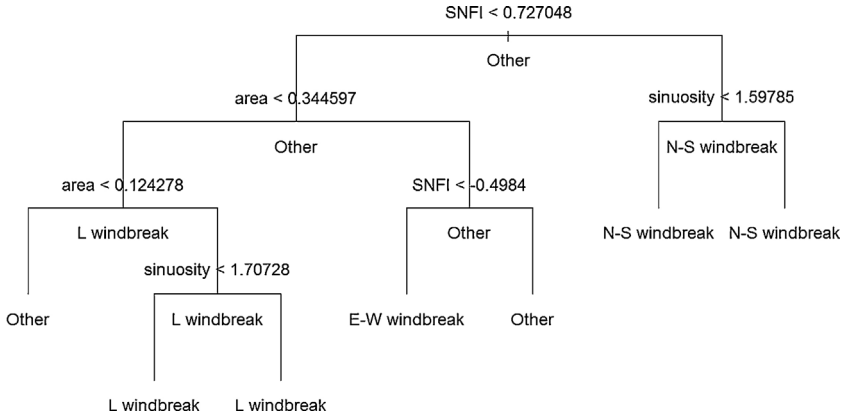

Fig. 10. A classification tree of three classes of windbreak, north–south windbreaks (N–S windbreak), east–west windbreaks (E–W windbreaks), L-shaped windbreaks (L windbreak), and non-windbreak features (Other) using three shape metrics – SNFI, sinuosity, and an area index.

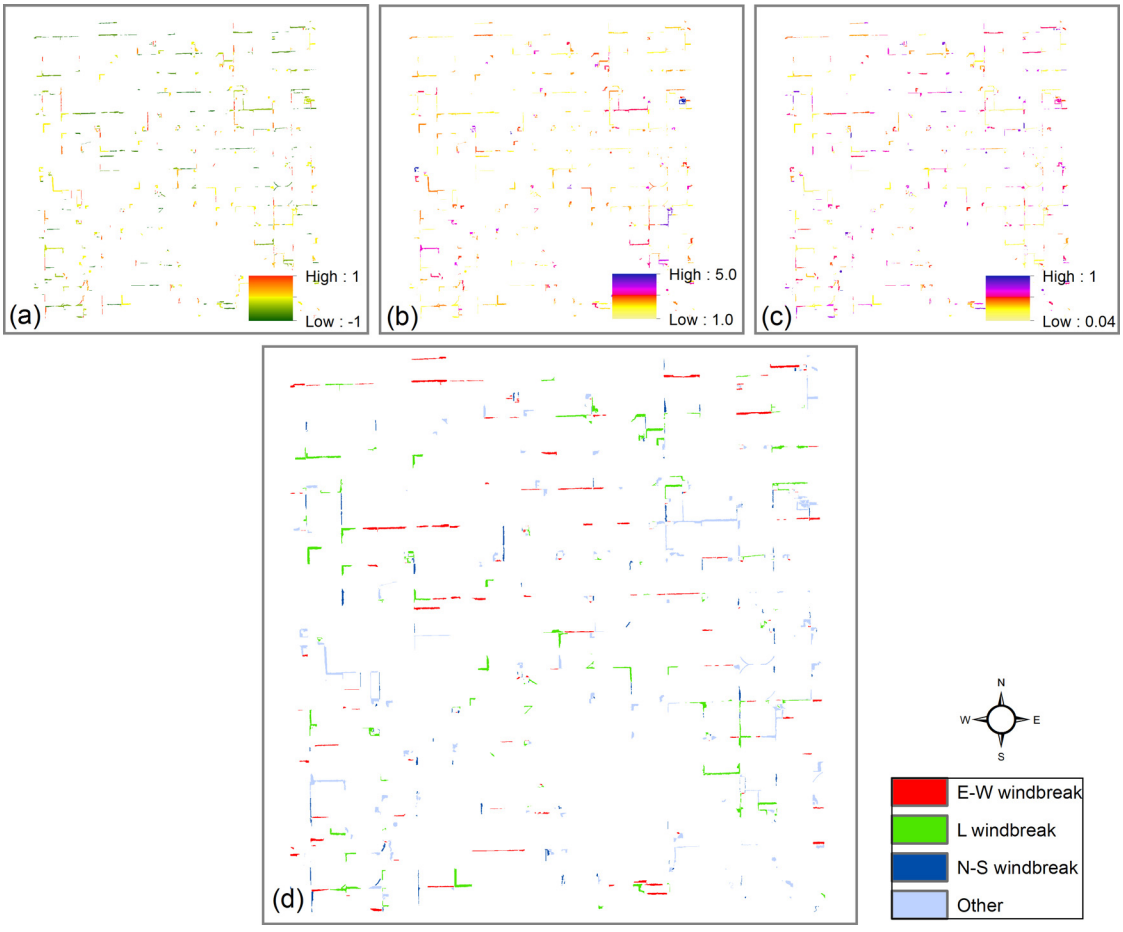

Fig. 11. Three shape indexes, SNFI (a), windbreak sinuosity (b), and area index (c) for tree features in a study area in Nebraska, USA. Four tree cover classes were labeled by a classification tree using the three shape indexes as inputs (d).

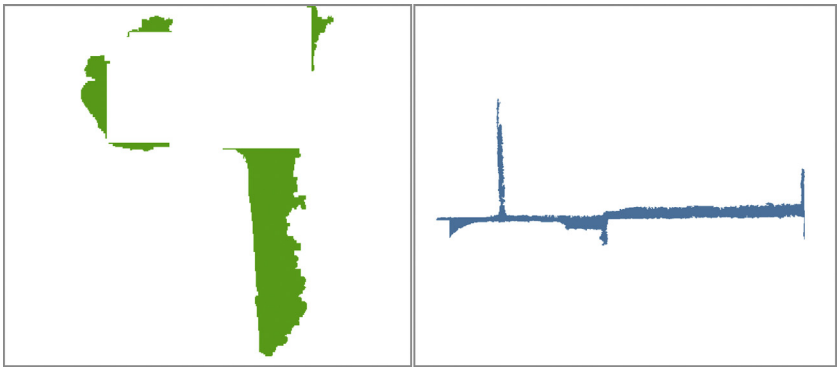

Fig. 12. Examples of tree-covered zones from study area 2 with questionable classification based on shape metrics. Tree covered areas surrounding a building (left) appear to be mostly linear, and were therefore identified as windbreaks. A windbreak has multiple L-shaped components (right) and was classified as "other" rather than an L-shaped windbreak.

94.3% (50/53) of the zones (Fig. 11). The classification tree struggled to correctly label features that may be the result of natural and planted features in close proximity (Fig. 12a) or features that may be combinations of straight-line and L-shaped windbreaks (Fig. 12b).

4. Discussion

Efficient methods for identifying windbreaks from raster data covering a large area are needed in order to facilitate comparisons between geographic locations and to monitor changes in the resource. Linear detection methods are focused on finding narrow features but not necessarily features that are straight. For example, Aksoy et al. (2010) applied a top-hat transformation to find candidate woody vegetation features within a certain range of widths; however, in order to determine which features were straight, further analysis was required. We examined alternatives to this approach by applying morphological methods and by exploiting information that can be calculated for contiguous groups of pixels (i.e., zones). The Straight and Narrow Feature Index (SNFI) presented here is calculated by counting pixels that remain in a zone after two erosions are applied separately in two directions and then constructing a normalized difference ratio from the zonal sum-

maries. Based on samples from two study areas in Nebraska, the index performs as expected with values near −1 for east–west windbreaks and values near +1 for north–south windbreaks.

We tested the ability of three shape metrics applied in two landscapes to distinguish between windbreaks and non-windbreaks. In the riparian study area, all three indexes provided significant separation between windbreak and non-windbreak features, as assessed by non-parametric statistical tests. A classification tree applied to the samples correctly categorized more than 90% of samples using SNFI or the sinuosity index alone. We note that using all available metrics in a classification tree did not improve accuracy. A conservative threshold could be selected for either SNFI or the sinuosity index as a first cut at detecting tree-cover features (zones) that could be windbreaks. The indexes struggled primarily with compact riparian features that were slightly elongated in one direction and had relatively smooth boundaries.

In the agricultural study area, we attempted to classify four classes of tree cover, and statistical tests indicate that all pairs of classes, except L-shaped windbreak vs. other, are separable using at least one of the shape indexes. Using classification trees, no single index classified samples correctly more than 85% of the time. However, in combination, the indexes correctly classified 94.3% of the samples. The indexes are designed to be complementary, each quantifying some characteristic of windbreaks, and this is a promising result. The relative values of the classes of tree cover were generally consistent between the two study areas but the values selected by the classification trees for splitting are tuned specifically to the samples and were not consistent among the study areas. However, the high degree of separability between tree cover classes with respect to the indexes indicates they can be a useful tool in windbreaks assessments based on raster data.

There are a number of methods in the machine vision literature designed to detect corners (e.g., Harris and Stephens, 1988). These approaches could reduce the confusion between L-shaped windbreaks and other tree cover. Other misclassifications occurred for tree cover patches that fall outside the conceptual model of windbreaks used to develop the indexes, such as combinations of basic windbreak shapes in a single, contiguous feature. Additional metrics that account for context (the spatial associations with other land cover classes) would help to address some of these challenging scenarios.

5. Conclusions

We present a new index termed the Straight and Narrow Feature Index (SNFI) that uses morphological erosion and zonal statistics to separate north–south and east–west linear windbreaks from other tree features. We also present complementary windbreak sinuosity and area indexes that can readily be calculated using raster functions, including zonal statistics. Users only need to specify a maximum expected width parameter in order to calculate SNFI and no parameters for the other two. The indexes can be useful tools to consumers of OBIA-derived datasets when shape-based information can help reveal additional information about features of interest, such as the use or function of contiguous patches on the landscape. The indexes were able to classify four classes of tree cover in an agricultural landscape (north–south windbreak, east–west windbreak, L-shaped windbreak, and other) with 94% accuracy. Additional work applying morphological concepts in different combinations and with context information could improve upon this methodology. These approaches hold excellent promise for parsing tree cover in existing land cover datasets into windbreaks, riparian corridors, and other functions in agricultural landscapes.

Appendix A. Supplementary data

Supplementary data associated with this article can be found, in the online version, at http://dx.doi.org/10.1016/j.jag.2017.03.005. These data include Google maps of the most important areas described in this article.

References

Aksoy, S., Akçay, H.G., Wassenaar, T., 2010. Automatic mapping of linear woody vegetation features in agricultural landscapes using very high resolution imagery. IEEE Trans. Geosci. Remote Sens. 48 (1), 511–522.

Basu, S., et al., 2015. A semiautomated probabilistic framework for tree-cover delineation from 1-m NAIP imagery using a high-performance computing architecture. IEEE Trans. Geosci. Remote Sens. 53 (10), 5690–5708.

Benediktsson, J.A., Pesaresi, M., Arnason, K., 2003. Classification and feature extraction for remote sensing images from urban areas based on morphological transformation. IEEE Trans. Geosci. Remote Sens. 41 (9), 1940–1949.

Brandle, J., Hodges, L., Zhou, X., 2004. Windbreaks in North American agricultural systems. Agroforestry Syst. 61, 65–78.

Breiman, L., 2001. Random forests. Mach. Learn. 45, 5–32.

Chanussot, J., Benediktsson, J.A., Fauvel, M., 2006. Classification of remote sensing images from urban areas using a fuzzy probabilistic model. IEEE Trans. Geosci. Remote Sens. 3 (1), 40–44.

Dougherty, E.R., Lotufo, R.A., 2003. Hands-on Morphological Image Processing. SPIE Press, Bellingham, WA.

Ghimire, B., Rogan, J., Miller, J., 2010. Contextual land-cover classification: incorporating spatial dependence in land-cover classification models using random forests and the Getis statistic. Remote Sens. Lett. 1 (1), 45–54.

Giraudoux, P., 2016. pgirmess: Data Analysis in Ecology. R package version 1.6.4, https://CRAN.R-project.org/package=pgirmess.

Harris, C., Stephens, M., 1988. A combined corner and edge detector. Proceedings of the 4th Alvey Vision Conference, 147–151.

Kettig, R.L., Landgrebe, D.A., 1976. Classification of multispectral image data by extraction and classification of homogeneous objects. IEEE Trans. Geosci. Electron. 14 (1), 19–26.

Liknes, G.C., Perry, C.H., Meneguzzo, D.M., 2010. Assessing tree cover in agricultural landscapes using high-resolution aerial imagery. J. Terr. Observ. 2 (1) (Article 5).

Meneguzzo, D.M., Liknes, G.C., Nelson, M.D., 2013. Mapping trees outside forests using high-resolution aerial imagery: a comparison of pixel- and object-based classification approaches. Environ. Monit. Assess. 185, 6261–6275.

Mueller, J., 1968. An introduction to the hydraulic and topographic sinuosity indexes. Ann. Assoc. Am. Geogr. 58 (2), 371, http://dx.doi.org/10.1111/j.1467-8306.1968.tb00650.x.

O'Connell, B.M., LaPoint, E.B., Turner, J.A., Ridley, T., Pugh, S.A., Wilson, A.M., Waddell, K.L., Conkling, B.L., 2014. The Forest Inventory and Analysis Database: Database Description and User Guide Version 6.0.1 for Phase 2. USDA For. Serv., Washington, DC, pp. 748.

Quackenbush, L.J., 2004. A review of techniques for extracting linear features from imagery. Photogramm. Eng. Remote Sens. 70 (12), 1383–1392.

Riitters, K.H., Vogt, P., Soille, P., Estreguil, C., 2009. Landscape patterns from mathematical morphology on maps with contagion. Landsc. Ecol. 24, 699–709.

Ripley, B., 2016. tree: Classification and Regression Trees. R package version 1.0-37, http://CRAN.R-project.org/package=tree.

Siegel, S., Castellan, N.J., 1988. Non Parametric Statistics for the Behavioural Sciences. MacGraw Hill Int., New York, pp. 213–214.

Soille, P., Vogt, P., 2009. Morphological segmentation of binary patterns. Pattern Recogn. Lett. 30, 456–459.

Sun, Z., Fang, H., Deng, M., Chen, A., Yue, P., Di, L., 2015. Regular Shape Similarity Index: a novel index for accurate extraction of regular objects from remote sensing images. IEEE Trans. Geosci. Remote Sens. 53 (7), 3737–3748.

U.S. Dept. of Agriculture, 2012. Working Trees for Agriculture, 7th ed, Accessed from http://nac.unl.edu/documents/workingtrees/brochures/wta.pdf (accessed 1.09.16).

van der Werff, H.M.A., van der Meer, F.D., 2008. Shape-based classification of spectrally identical objects. ISPRS J. Photogramm. Remote Sens. 63 (2), 251–258.

Vogt, P., Riitters, K., Iwanowski, M., Estreguil, C., Kozak, J., Soille, P., 2007. Mapping landscape corridors. Ecol. Indic. 7 (2), 481–488.